Thermodynamics analysis of a novel compressed air energy storage (CAES) system combined with SOFC-MGT and using low grade waste heat as heat source

Chen Yang [a, *], Li Sun [b],

[a] *Chongqing University, Shapingba District, Chongqing 400044, China*
yxtyc@cqu.edu.cn

Abstract

As modern societies face increasing energy demands and a complex smart grid with multiple inputs of traditional and intermittent renewable energy power generation systems, the need for energy storage systems has become a general trend. Among these systems, compressed air energy storage (CAES) has received extensive attention due to its low cost and high efficiency. This study proposes a novel design framework for a hybrid energy system comprised of CAES system, gas turbine, and high-temperature solid oxide fuel cells, aiming for power generation and energy storage solutions. The overall model of the hybrid power generation system was constructed in Aspen Plus, and the mass balance, energy balance, and thermodynamic properties of the thermal system were simulated and analyzed. The results demonstrate that the hybrid system utilizes the functional complementarity of CAES and solid oxide fuel cells (SOFC), resulting in the cascade utilization of energy, flexible operation mode and increased efficiency. The overall round trip efficiency of the system is 63%, and the overall exergy efficiency is 67%, with a design net power output of 12.5 MW. Additionally, thermodynamic analysis shows that it is advisable to operate the system under higher compressor and turbine isentropic efficiencies, and optimal SOFC/MGT(Micro Gas Turbine) split air flow rates. The results of this article provide guidance for designing innovative hybrid systems and system optimization.

1. Introduction

For nearly a century, the use of traditional fossil fuels has provided a stable and huge contribution to the progress of human civilization. But with a growing population and improved living standards, energy demand is expected to increase dramatically. According to statistics, it is estimated that by 2100, the global population will reach 10 billion. Meanwhile,emissions will increase correspondingly if immediate action is not taken. Looking at it today, the world emits about 51 billion tons of greenhouse gases into the atmosphere every year. In order to prevent climate disasters, countries around the world have established relevant policies and measures to reduce carbon emissions and strive to reduce carbon emissions to zero by 2050(IPCC,2022). This indicates that the most imminent and important task within the next three decades is to improve the efficiency of the existing energy systems, and to increase the share of renewable energy in the energy sector.

However, the utilization of renewable energy sources is accompanied by uncertainties and instabilities due to environmental factors such as wind and solar radiation. The integration of large-scale renewable energy into the power grid can have significant impacts on grid security and compromise the quality of electrical energy. This poses substantial challenges for maintaining power balance and ensuring stability control in the grid. To address these challenges, energy storage technologies have emerged as essential solutions. Energy storage technologies offer the capability for large and medium-scale energy storage and rapid response. When integrated into comprehensive energy systems that encompass conventional fossil fuel power generation and renewable energy sources, energy storage technologies play a pivotal role in maintaining power and energy balance across various operating conditions. Consequently, energy storage holds crucial implications for enhancing grid security, facilitating economic operation, and maximizing the utilization of renewable energy sources (Bazdar E et.al,2022).

Among various energy storage technologies, Advanced Adiabatic Compressed Air Energy Storage (AA-CAES) technology has gained significant attention from researchers in the past decade due to its advantages of large-scale energy storage, high energy efficiency, and zero emissions (Zhang, W.2020). However, the operation of AA-CAES requires the storage of compressed heat during the energy storage period the utilization of compressed heat to heat the air during the energy

release phase (G. Grazzini and A. Milazzo,2008). This characteristic imposes high requirements on the capacity, efficiency, and control of the heat exchangers and thermal storage systems. Therefore, in order to improve the overall efficiency of Compressed Air Energy Storage (CAES) and reduce emissions, one potential solution is to explore the utilization of other thermal sources within the comprehensive energy system to achieve better energy grade utilization (Javier, M,2019). In addition, the integration of different thermal sources within the comprehensive energy system allows for greater flexibility and versatility in energy generation and utilization. It enables the system to adapt to varying energy demands and optimize the use of available resources based on specific conditions or requirements. (Li Y, et al.2019).

In order to evaluate the potential of Compressed Air Energy Storage (CAES) in enhancing renewable energy integration, researchers have developed a comprehensive approach by merging a fixed efficiency model and a detailed thermoelectric model of CAES with unit commitment and economic dispatch algorithms (Nikolakakis, T, et al.2017).

SOFC can be well applied to large-scale distributed power generation systems of hundreds of megawatts. Typically, SOFC is operating at a high temperature range of 800-1000℃ with capabilities of high energy conversion rate, high current density and power density, wide fuel applicability, good electrode economy, modular assembly, and low emission. In particular, SOFC has strong reaction kinetics and is hardly poisoned by impurities such as CO and its by-products, so it has received widespread attention from researchers all over the world. However, commercially available solid oxide fuel cells (SOFCs) can only operate safely in steady-state mode, and therefore they need to be integrated with an energy storage system for use in load-following applications. Nease and Adams (2014a) proposed a coal-fueled SOFC plant integrated with compressed air energy storage (CAES) which had no CO2 emissions. And then they referred a two-stage rolling horizon optimization (RHO) framework is used to optimize a SOFC/CAES integrated power plant, achieving optimal year-round peaking power with zero emissions and significantly improving load-following performance by up to 90% (J. Nease and T.A. Adams II,2013) (Nease, J, et al.2016).

This study aims to figure out the interaction between a SOFC/MGT system and an AA-CAES system by considering the energy and exergy balance. The study also investigates the impact of different input parameters on novel system performance. The contributions of this work are summarized as below.

First, a new hybrid system is proposed in this paper, namely the AA-CAES system integrated with the SOFC/MGT system. Although there have been scholars who have done similar integrations in the past, but it is only a simple superposition, the system integration in this article is more thorough, and the combination between subsystems is more precise. This is mainly reflected in the thermal coupling between subsystems in this paper is designed based on the characteristics of each subsystem itself. That is to say, this paper not only realizes the cascade utilization of energy according to the difference of temperature, but also considers the safety and actual operation requirements of the subsystem. Moreover, unlike other similar systems, the CAES system in this paper is upstream of SOFC/MGT, addressing the pain points of the control problems caused by the interconnection of compressors and turbines and deep coupling with SOFC in traditional SOFC/MGT systems.

Secondly, when considering round trip efficiency and exergy efficiency in this paper, different analysis methods are proposed because of the time-segmented characteristics of energy storage systems. It considers not only the performance of the system under different operating modes, but also the intrinsic characteristics of different subsystems.

Finally, the impact of the study of key parameters on system performance can provide the goal of system optimization and also enhance the actual engineering value of the entire system.

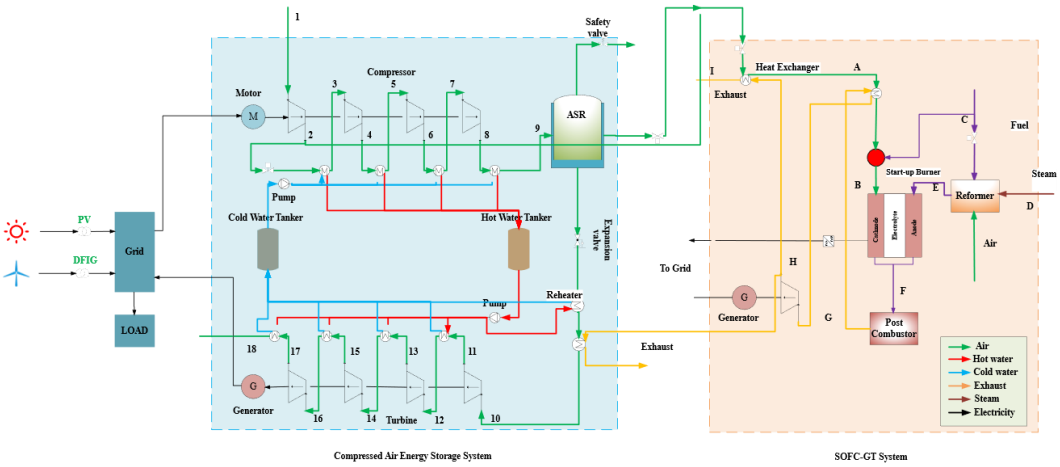

Figure 1. Overview of the CAES-SOFC/MGT Hybrid system

2. Methodology

It can be seen the working process of the integrated system used for this work from

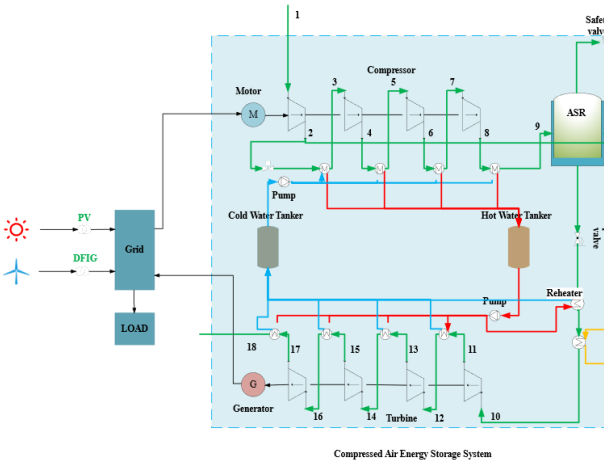

Figure *1*. Firstly, it is assumed that the SOFC-MGT system is always working as the base load. The hybrid power generation system combines compressed air energy storage, fuel cells, and a gas turbine. The system includes an air compressor unit, energy release turbine unit, heat storage tanks, gas storage tank, generator, motor, regenerator, and fuel cell power generation system. The motor drives the air compressor unit to compress air when surplus power is available. The compressed air is stored and released through the turbine group, connected to the generator. The fuel cell system is connected to the grid and includes a start-up burner, reactor, fuel cell body, afterburner, and post-combustion turbine. The high-pressure air from the compressor is heated by the microturbine exhaust for waste heat recovery before entering the fuel cell. In case of peak load, the compressors use the surplus electricity from renewable energy generation and compress the air into the storage tank in the charge mode. The stage inter cooling heat exchanges pump the heat into a hot water tank. Meanwhile, the first compressor of the charge chain works for SOFC. The compressed air without cooling supplies the cathode. Besides, before flowing into the fuel cell, the high-pressure air is heated by exhaust gas from the gas turbine, which can make the utmost of the wasted heat. The fuel cell generates the power to grid and the high pressure, temperature by-product with remain fuel flows into the turbine to generate power too. In the discharge mode, the air turbines are also working in four stages. The gases coming into the air turbines are heated up by the transfer fluid both in hot water tank and gas turbine. The cooling water goes to the cold water tank driven by the pump system.

Since the operation of the energy storage system has a time difference, in order to better analyze the operation of each component in each stage, this paper divides the operation of the entire system into five states, which can be seen from Figure *2*.

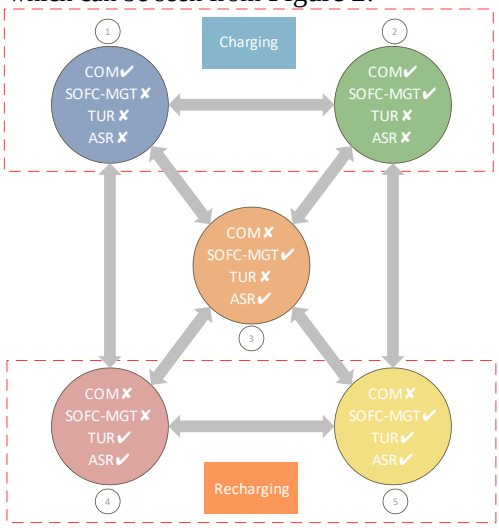

Figure 2. Working states of the CAES-SOFC/MGT Hybrid system.

In Figure 2, mode 1 to 5 represent the operating states of each subsystem, where the checkmark symbol indicates that the subsystem is running, and the cross symbol indicates that the subsystem is not running. Mode 2 and 5 represent the typical operating states of the system, while mode 1, 3, and 4 are used only in extreme conditions or for testing the system performance.

When the grid load is below the preset energy storage load, the grid functions as a motor to drive the air compressor unit, which compresses and stores the air in the gas storage device. During compression, the cold water from the tank's cold water tank flows into the heat exchanger to cool the compressed air, and then flows into the hot water tank.

Mode 1 is a test mode used to detect the working mode of the compression chain when it runs alone. At this mode, the air storage reservoir is in the energy storage stage, while other subsystems are inactive.

Mode 2 is the normal energy storage mode of the system. At this mode, excess power from the grid drives the compressor to produce compressed air. Some of the compressed air is stored in the air tank, while the rest is used as the cathode inlet air of the fuel cell, serving as the SOFC-MGT air source.

Mode 3 is a test mode and also the minimum output power condition of the system, which is used to test the working mode of the SOFC-MGT system when it is running alone. In this mode, the air tank serves as the air source of the SOFC-MGT system, and the compressed air is used as the cathode inlet of the fuel cell. When the air tank is fully charged, the SOFC-MGT system can provide compressed air to the entire system for hours or even days, depending on its capacity. Therefore, this mode can be used as a reference for black start situations, where the energy storage system provides users with the minimum necessary output power when the external power grid is paralyzed.

Mode 4 is designed as a test mode to evaluate the energy release chain's working status when it operates independently. In this mode, the compressed air from the air tank is supplied to the air turbine, and the hot water in the hot water tank and the regenerator between each stage heat the compressed air. This process allows the compression heat in the compression stage to be fully utilized.

Mode 5 represents the normal energy release mode and the maximum output power of the system. In this mode, the compressed air in the air tank is split into two streams, of which one stream directly drives the air turbine to generate electricity, while the other stream serves as the anode inlet air for the SOFC-MGT system. Unlike mode 4, the high-temperature exhaust gas at the outlet of the SOFC-MGT system heats the inlet air of the first-stage air turbine, allowing for the full utilization of the waste heat from the exhaust gas.

The following assumptions are made to simplify the whole system modeling.

(1) The composition of air in CAES system and SOFC cathode inlet consists of 79% N_2 and 21% O_2 (mass fraction).
(2) The heat and pressure loss in the pipes connecting all the components can be negligible.
(3) All the kinetic and potential effects are ignored.
(4) The storage tank is adiabatic during the charging and discharging process.
(5) The water gas reaction is in a state of chemical equilibrium.
(6) The effect of radiation heat transfer is not considered.
(7) The system operates under steady state conditions.
(8) The isentropic efficiency of each compressor and turbine is fixed.

Basic geometric and operating parameters of this hybrid system are shown in Table 1 and

System parameters	Value
Ambient pressure / bar	1.000
Ambient temperature / k	298.0
Maximum pressure of ASR /bar	100
Minimum pressure of ASR /bar	70
Volume of the air tank /m^3	6000
Hot water tank temperature / k	403.0
Hot water tank pressure / bar	4.000
Cold water tank temperature / k	298.0
Cold water tank pressure / bar	1.000
Generator efficiency	0.98
Inlet pressure / bar	70.00

Table *2*. The SOFC geometric parameters were taken from (Huang S, et al.2022):

Table 1. Basic operating parameters for CAES

System parameters	Value
Ambient pressure / bar	1.000
Ambient temperature / k	298.0
Maximum pressure of ASR /bar	100
Minimum pressure of ASR /bar	70
Volume of the air tank /m^3	6000
Hot water tank temperature / k	403.0
Hot water tank pressure / bar	4.000
Cold water tank temperature / k	298.0
Cold water tank pressure / bar	1.000
Generator efficiency	0.98
Inlet pressure / bar	70.00

Table 2.Operating parameters for SOFC/GT hybrid system

Operating parameters	Value
Total cell area	200.0×200.0 mm
Anode thickness	0.5 mm
Electrolyte thickness	0.008 mm
Cathode thickness	0.05 mm
Number of channels	50
Channel size	2.0×2.0 mm^2
Cathode inlet pressure	3.9 bar
Anode inlet pressure	3.9 bar
Average SOFC temperature	939 °C
Current density	0.676 A/cm2
Fuel utilization factor	0.62
Reformer inlet composition (molar fraction)	33% CH_4, 67% H_2O
Turbine isentropic efficiency	86%
Turbine mechanic efficiency	98%

2.1 Compressor

There are four air compressors in the system connected in series, with interstage coolers between each compressor, and an aftercooler after the fourth air compressor. The outlet pressure of the air compressor can be calculated by the following formula (Hartmann N, et al. 2012):

$$P_{out,c} = \pi_c P_{in,c} \tag{1}$$

where $P_{in,c}$ is the inlet pressure of the compressor, π_c is the compression ratio of the air compressor, and the inlet pressure of the first stage compressor is atmospheric pressure. The outlet temperature of the compressor is:

$$T_{out,c} = T_{\mathrm{in},c}[1+(\pi_c^{(\mathrm{k}-1)/\mathrm{k}}-1)/\lambda_c] \tag{2}$$

where $T_{\mathrm{in},c}$ is the inlet temperature and λ_c is the isentropic efficiency of the compressor. k is the specific heat ratio. The power consumed by the compressor is:

$$\begin{aligned}\dot{\mathrm{W}}_{com} &= \dot{m}_{c,in}(\mathrm{h}_{c,out}-\mathrm{h}_{c,\mathrm{in}}) \\ &= C_{\mathrm{p}}\dot{m}_{c,in}T_{\mathrm{in},c}\frac{1}{\eta_c}(\pi_c^{(k-1/k)}-1)\end{aligned} \tag{3}$$

where $\dot{m}_{c,in}$ is the inlet air mass flow rate of the air compressor in the energy storage stage, $\mathrm{h}_{c,out}$ and $\mathrm{h}_{c,\mathrm{in}}$ are the specific enthalpy of the outlet and inlet air, respectively.

2.2 Heat exchanger

The heat of compression is transferred to the heat storage device through the interstage heat exchanger, and a counter-flow heat exchanger is used in this paper. The water temperature is approximately equal to ambient temperature before entering the interstage cooler. From the law of conservation of energy （Guo C, et al. 2017）.

$$\begin{aligned}&\dot{m}_{c,\mathrm{air}}(\mathrm{h}_{\mathrm{int}er,air,in}-\mathrm{h}_{\mathrm{int}er,air,\mathrm{out}}) \\ &= \dot{m}_{c,\mathrm{water}}(\mathrm{h}_{\mathrm{int}er,\mathrm{water,out}}-\mathrm{h}_{\mathrm{int}er,\mathrm{water,in}}) = \mu_{\mathrm{int}er}A_{\mathrm{int}er}\Delta T_{\mathrm{int}er}\end{aligned} \tag{4}$$

Where $\mathrm{h}_{\mathrm{int}er,air,in}$ and $\mathrm{h}_{\mathrm{int}er,air,\mathrm{out}}$ are the air specific enthalpy at the inlet and outlet of the interstage cooler, $\mathrm{h}_{\mathrm{int}er,\mathrm{water,out}}$ and $\mathrm{h}_{\mathrm{int}er,\mathrm{water,in}}$ are the specific enthalpy of the water in the heat storage system at the inlet and outlet of the interstage cooler, $\mu_{\mathrm{int}er}$ is the thermal conductivity of the heat exchanger, and $A_{\mathrm{int}er}$ is the heat transfer area, $\Delta T_{\mathrm{int}er}$ is the logarithmic mean temperature difference between air and water.

There is a regenerator in front of each turbine, which is the same as the energy storage part, which is a counter-flow heat exchanger. In the regenerator, the hot water stored in the hot water tank is heated to the air flowing out of the air storage tank, and then in the cold water tank was cooled to room temperature.

$$\dot{m}_{c,\mathrm{air}}(\mathrm{h}_{\mathrm{re},air,out}-\mathrm{h}_{\mathrm{re},air,\mathrm{in}}) = \dot{m}_{c,\mathrm{water}}(\mathrm{h}_{\mathrm{re,water,in}}-\mathrm{h}_{\mathrm{re,water,out}}) \tag{5}$$

where $\mathrm{h}_{\mathrm{re},air,\mathrm{in}}$. and $\mathrm{h}_{\mathrm{re},air,out}$ are the specific enthalpy of air at the inlet and outlet of the regenerator, and

$h_{re,water,in}$ and $h_{re,water,out}$ are the specific enthalpy of water at the inlet and outlet of the regenerator.

2.3 Turbine

In this paper, four turbines are connected in series. The outlet pressure of the turbine can be calculated by the following formula (Hartmann N, et al. 2012)(Guo H, et al.2019):

$$P_{\mathrm{in,t}} = \pi_t P_{\mathrm{out,t}} \tag{6}$$

where $P_{\mathrm{in,t}}$ is the inlet pressure of the turbine, π_t is the expansion ratio of the turbine, and the inlet pressure of the first stage turbine is the outlet pressure of the gas storage tank. The outlet temperature of the turbine is:

$$T_{out,\mathrm{t}} = T_{\mathrm{in,t}}[1-\lambda_t(1-\pi_t^{(\mathrm{k}-1)/\mathrm{k}})] \tag{7}$$

where $T_{\mathrm{in,t}}$ is the inlet temperature of the turbine, and λ_t is the isentropic efficiency of the turbine. *k* is the specific heat ratio. Turbine work can be calculated by the following formula:

$$\begin{aligned}\dot{\mathrm{W}}_t &= \dot{m}_{\mathrm{t,air}}(\mathrm{h}_{\mathrm{t,in}} - \mathrm{h}_{c,\mathrm{out}}) \\ &= C_{\mathrm{p}}\dot{m}_{\mathrm{t,air}}T_{\mathrm{in,t}}\lambda_{\mathrm{t}}(\pi_t^{(k-1/k)}-1)\end{aligned} \tag{8}$$

2.4 Air storage tank

After flowing out of the interstage cooler, the hot water absorbing the heat of compression will be stored in the hot water tank.

In this paper, the gas storage device adopts the gas storage tank. In order to study the performance of the gas storage tank, according to the law of mass conservation and energy conservation (Wu S,et al.2019):

$$\begin{aligned}&Q_{\tan k} = \dot{m}_{c,in}h_{c,in} - \dot{m}_{t,out}h_{t,out} \\ &-\dot{m}_{\mathrm{split},out}h_{\mathrm{split},out} - Q_{\mathrm{loss}}\end{aligned} \tag{9}$$

$$m_{\tan \mathrm{k}} = \dot{m}_{\mathrm{c},in}\mathrm{t}_c - \dot{m}_{t,out}t_t - \dot{m}_{split,out}t_t \tag{10}$$

where $Q_{\tan k}$ and Q_{loss} is the rate of transferred heat, $\dot{m}$ is the air flow rate, t_c and t_t is the charge time and discharge time, and the subscript split represents air split from tank in the mode 5.

2.5 SOFC/MGT

The SOFC model used the lumped parameter method to calculate the local current density, distribution temperature distribution, Nernst potential, and electrochemical loss of the whole fuel cell. The chemical kinetic model was used to calculate the water gas shift reaction, steam methane reforming reaction, and electrochemical reaction. The SOFC model was created in ACM and imported into Aspen Plus TM. The current density can be calculated based on the feed flow rate of each component of the inlet fuel and the set fuel utilization rate. The operating conditions of the fuel cell are modeled in terms of inlet and outlet average temperatures, pressures, and stream composition. The cell voltage is calculated by Bulter-Volmer formula, and the power output of a fuel cell can be calculated based on the total reaction area of the cell and the total number of cells. Thomas Paul Smith et al. published a detailed description of the model and validation work. The electrochemical loss and cell voltage calculations are expressed by equations as follows (Liese E A, et al. 2006).

$$V_{cell} = V_{Nernst} - \eta_{act} - \eta_{con} - \eta_{ohm} \tag{11}$$

$$V_{Nernst} = E^0 + \frac{RT}{2F}\ln[\frac{P_{H_2}P_{O_2}^{0.5}}{P_{H_2O}}] \tag{12}$$

$$E^0 = 1.2877 - 0.0002904T_{cell,bulk} \tag{13}$$

$$\eta_{\mathrm{con}} = \frac{RT}{2F}\left(\ln(\frac{\chi_{H_2,bulk}\chi_{H_2O,TPB}}{\chi_{H_2O,bulk}\chi_{H_2,TPB}})\right) + \frac{1}{2}\ln(\frac{\chi_{H_2,bulk}}{\chi_{O_2,TPB}}) \tag{14}$$

$$\eta_{act} = \frac{RT}{2\alpha F}\sinh^{-1}\left(\frac{i}{2i_o}\right) \tag{15}$$

$$\eta_{ohm} = \left[\begin{array}{l}6.78E-10\exp(\frac{10.3E3}{T_{cell,bulk}}) + \\ 0.23174\exp(-0.0115T_{cell,bulk})\end{array}\right] * i \tag{16}$$

This paper uses the ACM model in the Aspen Plus software model library to establish the SOFC battery model. Before flowing into the cathode, a part of the air is split into reformer, combusted with part of the fuel to make the reformer an autothermal reformer and ensure the temperature of the fuel at the anode inlet. The remaining air is discharged after exchanging heat with SOFC's outlet flue gas in the heat exchanger, while ensuring the inlet temperature of the after burner. At the anode, the natural gas undergoes a reforming reaction; the produced hydrogen reacts electrochemically with the air from the cathode to generate electricity.

The input data for natural gas, air volume, and water vapor required for the stack model were determined by the calculator model of the ASPEN plus. Assuming that the cells in the stack are connected in parallel, the voltage of each battery is the same. The current of the fuel cell stack is equal to the current per cell multiplied by the number of cells, which calculated in the SOFC ACM model.

2.6 Round trip efficiency

When dealing with a hybrid power system that includes an energy storage system, it can be challenging to determine a precise efficiency value, as the charging and discharging periods operating at divergent times. In such cases, the system's round-trip efficiency (RTE) is used as a metric. RTE is ratio of total electrical energy output to the total fuel and electrical energy input for a full charge/discharge cycle and can be calculated using the following formula:

$$RTE = \frac{\int_T W_{OUT}}{\int_T W_{IN}} = \frac{\int_{T_{dc}} W_t + \int_{T_{all}} (W_{MGT} + W_{SOFC}) + Q_{HL}}{\int_{T_{ch}} W_c + \int_{T_{all}} (\dot{m}_{CH_4} \cdot LHV_{CH_4})} \quad (17)$$

Where W_{OUT} is the electricity out , W_{IN} is the energy input, W_t is the electricity generation for expanders, W_{MGT} is the electricity generation for turbine, Q_{HL} is the excess heat load in hot water tank for end user. W_{SOFC} is the electricity generation for SOFC, W_{c} is the electricity consumption of compressors, $\dot{m}_{CH_4}$ is the mass flow of inlet CH_4 , LHV_{CH_4} is the lower heating value of CH_4 , T_{dc} is the discharge time, T_{ch} is the charge time, T_{all} is the one-cycle time.

2.7 Total exergy efficiency

Similar to the definition of system cycle efficiency, total exergy efficiency (TEE) is defined as the total net exergy output E_{xout} in discharging process to total net exergy input E_{xin} in the charging process. As the heating exergy is not considered in the reference, TEE can be presented as:

$$TEE = \frac{E_{xout}}{E_{xin}} = \frac{E_{xTB} + E_{xSOFC} + E_{xMGT}}{E_{xCOM} + E_{xCH4}} \quad (18)$$

where E_{xTB} is the total exergy of expanders, E_{xCOM} is the total exergy of compressors, E_{xSOFC} is the total exergy of SOFC, E_{xMGT} is the total exergy of turbine and E_{xCH4} is the total exergy of fuel.

3. Results and discussion

3.1 Influence of outlet pressure of expansion valve

In discharging process, the air from the ASR passes through the expansion valve so that a specific pressure will be set, which makes the turbines operate at the steady and high efficiency conditions. The changing of the required pressure has a direct influence on the turbines' performance. The power output of the turbine and the mass flow rate of air increase with increasing pressure behind the expansion valve. However, the operating range of the turbine narrows, and the discharge time decreases sharply. The 0-D system model lacks a control mechanism, resulting in changes in mass flow rate in response to pressure variations. As shown in Figure 3, modes 4 and mode 5's efficiencies rise with increasing post-valve pressure. The throttle valve has no impact on the operation of the compression chain and SOFC/MGT subsystems. Hence the efficiencies of modes 1, 2, and 3 remain unchanged. As pressure behind the valve rises gradually, the system RTE drops from 65.9% to 49.6%. The reason is that although the turbine does more work per unit of time, but the release time for energy decreases, which reduces the working range of the air storage tank, ultimately decreasing the total work done by the turbine.

Figure 4 shows the effect of expansion valve outlet pressure on the total exergy efficiency. In the figure, nECOM represents the exergy efficiency of the compressor, nETUR represents the exergy efficiency of the expander, nESOFC-MGT represents the exergy efficiency of SOFC-MGT, and EXALL represents the exergy efficiency of the system total exergy efficiency. As seen from Figure 4, the TEE of the compressor chain and SOFC/GT subsystem keep constant as well. But turbine chain subsystem's TEE increases with the varying expansion valve outlet pressure from 60 bar to 80 bar. It is evident that when the inlet pressure is increased, each turbine performs more work, leading to an increase in exergy efficiency. While the flow rate also rises, requiring more hot water heat and leading to greater exergy loss in the turbine chain's regenerator, these effects are relatively minor in comparison to the gain in exergy efficiency resulting from the increased work done by the turbines. However, TEE exhibits a clear downward trend. This is due to the significant reduction in the energy release time, despite the increase in work done per unit time by the turbine. Compared to the aforementioned effects, the energy discharge time has a greater impact on the total output exergy. In conclusion, the highest achievable values of the overall system's round trip efficiency and exergy efficiency are obtained when the heat load output to the user approaches zero, while the turbine maximizes the use of the compression heat and SOFC/MGT exhaust waste heat.

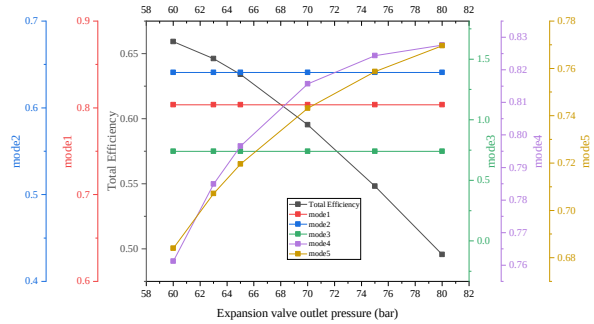

Figure 3. Effect of expansion valve outlet pressure on RTE

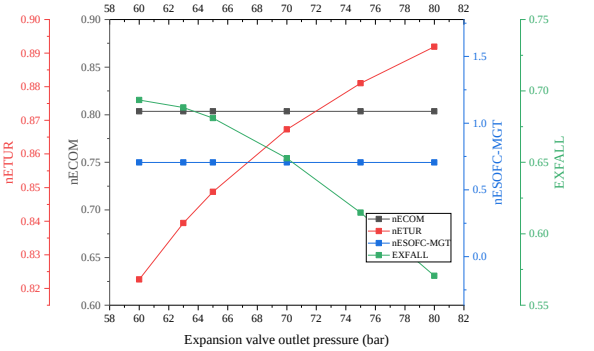

Figure 4. Effect of expansion valve outlet pressure on TEE

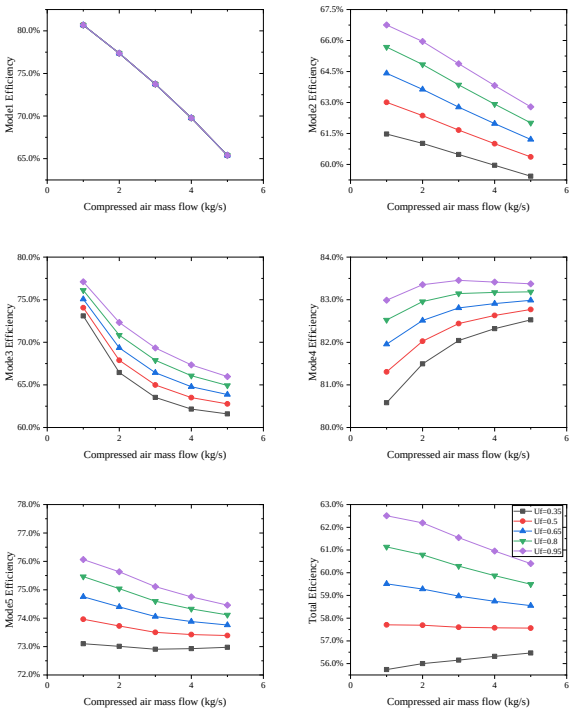

Figure 5. Energy flow diagram of CAES-SOFC/MGT Hybrid system

3.2 Influence of fuel utilization factor and air mass flow to SOFC/MGT system

Figure 5 presents a comprehensive analysis of the impact of varying the fuel utilization factor and SOFC/MGT air inlet mass flow on the efficiency of the hybrid system in different operating modes. Specifically, the figure demonstrates the effect of changing the aforementioned parameters on the overall efficiency of the hybrid system as well as the efficiencies of the individual subsystems in different operating modes.

As illustrated in Figure 5(a), the compressed air flow rate is the main factor affecting mode 1, which refers to the compression chain of the CAES system. When the compressed air flow rate diverted to the SOFC/MGT system increases, the flow rate of the compressor decreases. Consequently, the power consumption of stages 2-4 of the compressor decreases, along with a reduction in the compression heat. However, this also leads to a significant decrease in the energy stored per unit time, resulting in a reduction in the efficiency of mode 1. Because the efficiency reduction of the compressor is so large that even though the efficiency of the SOFC/MGT system has increased caused by the Uf(fuel utilization) changing, the efficiency in mode 2 is still reduced, but a higher Uf will result in higher efficiency, as shown in Figure 5(b). The efficiency of mode 3 is directly affected by the variation in Uf and the SOFC/MGT inlet flow rate. A high fuel utilization rate can reduce the fuel cell efficiency, and a large anode air flow can lower the average temperature of the fuel cell. However, since the compressed air in mode 3 mainly comes from the CAES subsystem's compressor, high fuel utilization rate leads to higher efficiency in mode 3. On the other hand, an increase in SOFC anode air reduces the heat output from the SOFC/MGT subsystem to the downstream, resulting in a decrease in efficiency. As shown in Figure 5(d), the increase in system efficiency is observed only at the energy release end of the CAES system. This is because the work done by the turbine per unit time remains unchanged, but the heat output to the turbine decreases. Combining the turbines with the SOFC/MGT, it can be seen that the efficiency reduction of the SOFC/MGT subsystem has a greater impact, so the efficiency under mode 5 is reduced.

Overall, the hybrid system's efficiency increases as fuel utilization increases, considering the changes in energy storage and release times due to variations in air flow. When fuel utilization is low, the SOFC/MGT subsystem's air flow has a positive effect on RTE. However, at high fuel utilization rates, the SOFC/MGT subsystem's air flow has a negative effect on RTE.

Figure 6 depicts the exergy efficiency of each subsystem and the overall system as a function of Uf

and the inlet air flow rate to the SOFC/MGT subsystem, while Figure 7 shows the variation of exergy loss of each main component and its proportion in the system under different combinations of Uf and inlet air flow rate. In these figures, Uf varies between 0.35 and 0.95, and the inlet air flow rate changes from 1kg/s to 5kg/s. The performance of the SOFC is strongly affected by Uf, which, in turn, impacts the performance of downstream components, such as the afterburner, MGT, and turbine chain. As shown in Figure 6, the exergy efficiency of the SOFC/MGT subsystem increases with Uf since a higher fuel utilization rate results in higher hydrogen reacting in the SOFC and, consequently, higher electric energy output. Additionally, the outlet temperature of the fuel cell is also higher, which reduces the combustible gas entering the combustion chamber downstream, leading to a reduction in the exergy loss of the combustion chamber. Consequently, the exergy loss of the MGT also decreases, and the degree of decrease has little effect on the decrease of the MGT's output work compared to the increase of the output work brought by the increase in the turbine inlet flow. The highest exergy efficiency of the solid SOFC/MGT subsystem is achieved when Uf is 95% and the inlet air flow rate is 5kg/s.

When the air flow to the SOFC/MGT subsystem increases, the flow rate of the 2-4 stage compressors in the compression chain of the CAES system decreases, and the power consumption also decreases, leading to a significant reduction in the compression heat of the entire compression chain. Furthermore, the exergy loss of the interstage cooler is reduced. As a result, the total exergy efficiency of the compression chain increases with an increase in the air flow diverted to the SOFC/MGT system. However, after a complete cycle, the split air flow rate reaches 5kg/s, and the difference between the heat of compression and the heat required for expansion of the entire system is negative, indicating that the system can no longer operate completely without additional external heat supply.

For the energy release chain of CAES, the input work of the turbine remains unchanged since the turbine inlet temperature and air flow rate remain constant. However, due to the reduction of the exhaust gas temperature of the SOFC/MGT system, the exergy loss of the heat exchanger between the compressed gas tank and the turbine chain is reduced, and the exergy efficiency of the solid-release energy chain slightly increases.

Based on the analysis above, combined with Figure 7, it can be concluded that for the entire hybrid system, the compression chain exergy loss of CAES is more sensitive to air flow changes, while SOFC/MGT has little effect on the exergy loss of the entire system. Therefore, the highest total exergy efficiency is 67.24%, which increases with the increase of Uf and inlet air flow rate of SOFC/MGT.

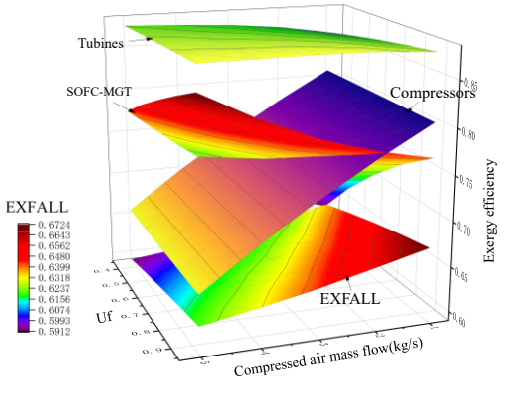

Figure 6. Effect of variation SOFC/MGT Uf and Inlet Air Mass Flow on TEE

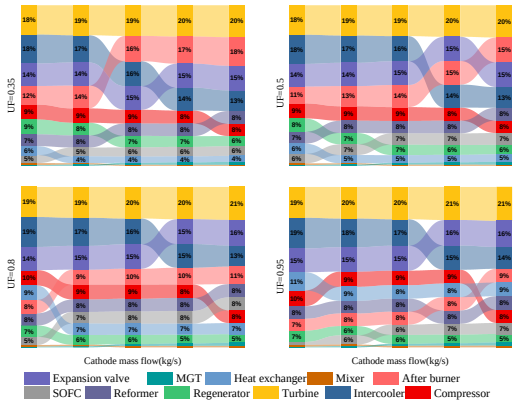

Figure 7. Percentage contribution of exergy destruction by each component with rise air mass flow to SOFC/MGT subsystem at varying fuel utilization factors.

4. Conclusions

This study presents a thermodynamic analysis of a novel hybrid CAES/SOFC/MGT generation system. A reliable static model of the system was established using ASPEN Customer Modeler and ASPEN Plus, and simulation experiments were conducted on key parameters to investigate the operating conditions of different subsystems and the overall system, in order to establish a reliable power generation and energy storage system. The following are some of the main results:

1. The influence of different parameters on the performance of hybrid system was evaluated by a parametric analysis. The study's findings suggest that to enhance the system's RTE and TEE, it is advisable to operate the system higher compressor and turbine isentropic efficiencies and optimal SOFC/MGT split air flow rates. These findings can be employed in future system design and modeling endeavors to perform multi-objective optimization, leading to superior system performance.

2. The effects of changes in multiple key system input parameters on efficiency and exergy efficiency were analyzed under different working modes and subsystems, which can better help to perform individual optimization of the actual operating conditions of the entire system.

The results offer valuable insights into the optimal operating conditions and design parameters for the system and can aid in the development of more efficient and cost-effective energy storage and generation solutions. Nevertheless, the static analysis approach proposed in this study provides valuable guidance for future system improvement and optimization. Furthermore, the model results obtained in this study not only serve as a valuable data source for dynamic model establishment, but also lay a foundation for multi-objective optimization of the system. Therefore, the value of system designed parameters should be selected wisely. Moreover, based on the findings of this study, the commercial potential of the system warrants further exploration.

Acknowledgment

This work was supported by the National Natural Science Foundation of China. (Grant number [51876011]).

Nomenclature

Abbreviations

CAES	Compressed air energy storage
SOFC	Solid oxide fuel cell
MGT	Micro gas turbine
AFC	Alkaline fuel cell
PAFC	Phosphoric acid fuel cells
MCFC	Molten carbonate fuel cell
PEMFC	Proton exchange membrane fuel cell
DMFC	Direct-methanol fuel cells
A-CAES	Adiabatic compressed air energy storage
AA-CAES	Advanced adiabatic compressed air energy storage
I-CAES	Isothermal compressed air energy storage
D-CAES	Diabatic compressed air energy storage

Parameters

P	Pressure (Pa)	Uf	Fuel utilization
T	Temperature(K)	E	Potential (V)
W	Work(J)	R	Molar gas constant ($J \cdot K^{-1} \cdot mol^{-1}$)
EX	Exergy (kW)	F	Faraday constant ($C \cdot mol^{-1}$)
h	enthalpy ($kJ \cdot kg^{-1}$)	i	Current density (A/cm^2)
π	Compression ratio	**Subscripts**	
k	Specific heat ratio	*out*	Outlet
m	Mass flow (kg/s)	*in*	Inlet
C_p	Heat capacity at constant pressure （J/K）	*c*	Compressor
Q	Amount of heat (kJ)	*inter*	Intercooler
λ	Efficiency	*re*	Regenerator
A	Area (m^2)	*t*	Turbine
μ	Thermal conductivity (W/m·K)	*Nernst*	Nernst Potential
V	Voltage (V)	*act*	Activation
η	Polarization loss(V)	*con*	Concentration
X	Mole fraction	*ohm*	Ohmic
α	Transmission coefficient	*split*	Split after 1st compressor
I	Exergy loss (kW)		

References

IPCC, (2022), Climate Change 2022: Mitigation of Climate Change. Contribution of Working Group III to the Sixth Assessment Report of the Intergovernmental Panel on Climate Change ,P.R. Shukla, J. Skea, R. Slade, A. Al Khourdajie, R. van Diemen, D. McCollum, M. Pathak, S. Some, P. Vyas, R. Fradera, M. Belkacemi, A. Hasija, G. Lisboa, S. Luz, J. Malley, (eds.). Cambridge University Press, USA. doi: 10.1017/9781009157926

Bazdar E, Sameti M, Nasiri F, et al. (2022) 'Compressed air energy storage in integrated energy systems: A review', *Renewable and Sustainable Energy Reviews*, pp. 167: 112701. doi: doi: 10.1016/j.rser.2022.112701.

Zhang, W., Xue, X., Liu, F., et al. (2020) 'Modelling and experimental validation f advanced adiabatic compressed air energy storage with off-design heat exchanger', *IET Renewable Power Gener*. 14, pp. 389–398. doi: 10.1049/iet-rpg.2019.0652.

G. Grazzini and A. Milazzo. (2008) 'Thermodynamic analysis of CAES/TES systems for renewable energy plants', *Renewable Energy*, vol. 33, pp.1998-2006. doi: 10.1016/j.renene.2007.12.003.

Javier, M., Ordóñezb, A., Álvarezb, R., et al. (2019) 'Energy from closed mines:underground energy storage and geothermal applications', *Renew. Sust.Energy Rev*, pp. 498–512. doi: 10.1016/j.rser.2019.04.007.

Li Y, Miao S, Yin B, Han J, Zhang S, Wang J, Luo X. (2019) 'Combined heat and power dispatch considering advanced adiabatic compressed air energy storage for wind power accommodation', *Energy Convers Manag*ement.pp 200: 112091. doi: 10.1016/j.enconman.2019.112091.

Nikolakakis, T., Fthenakis, V. (2017) 'The value of compressed-air energy storage or enhancing variable-renewable-energy integration: the case of Ireland',*Energy Technol*, pp. 2026–2038. doi: 10.1002/ente.201700151.

J. Nease and T.A. Adams II.(2014) '2014a, Coal-fuelled systems for peaking power with 100% CO2 capture through integration of solid oxide fuel cells with compressed air energy storage', J.*Power Sources*, pp. 92-107. doi: 10.1016/j.jpowsour.2013.11.040.

Nease, J., Monteiro, N., & Adams II, T. A. (2016). 'Application of a multiple time-scale rolling horizon optimization technique for improved load-following of an integrated SOFC/CAES plant with zero emissions', *In Computer Aided Chemical Engineering* , pp. 1725-1730. doi: 10.1016/b978-0-444-63428-3.50292-7.

Huang S, Yang C, Chen H, et al.(2022) 'Coupling impacts of SOFC operating temperature and fuel utilization on system net

efficiency in natural gas hybrid SOFC/GT system', *Case Studies in Thermal Engineering*, pp. 101-118. doi: 10.1016/j.csite.2022.101868.

Hartmann N, Vöhringer O, Kruck C, et al.(2012) 'Simulation and analysis of different adiabatic compressed air energy storage plant configurations', *Applied Energy*, pp. 541-548. doi: 10.1016/j.apenergy.2011.12.007.

Guo C, Xu Y, Zhang X, et al. (2017) 'Performance analysis of compressed air energy storage systems considering dynamic characteristics of compressed air storage', *Energy*, pp. 876-888. doi: 10.1016/j.energy.2017.06.145.

Guo H, Xu Y, Zhang Y, et al.(2019) 'Off-design performance and an optimal operation strategy for the multistage compression process in adiabatic compressed air energy storage systems', *Applied Thermal Engineering*, pp.262-274. doi: 10.1016/j.applthermaleng.2018.12.035.

Wu S, Zhou C, Doroodchi E, et al.(2019) 'Thermodynamic analysis of a novel hybrid thermochemical-compressed air energy storage system powered by wind, solar and/or off-peak electricity'. *Energy Conversion and Management*, pp.1268-1280. DOI: 10.1016/j.enconman.2018.11.063

Liese E A, Gemmen R S, Smith T P, et al.(2006) 'A dynamic bulk SOFC model used in a hybrid turbine controls test facility',*Turbo Expo: Power for Land, Sea, and Air*,pp.117-126. doi: 10.1115/gt2006-90383